Polymer 42 (2001) 4153–4162

polymer

www.elsevier.nl/locate/polymer

Kinetic modeling of methyl methacrylate free-radical polymerization initiated by tetraphenyl biphosphine

M. Krajnc*, I. Poljanšek, J. Golob

Faculty of Chemistry and Chemical Technology, University of Ljubljana, Aškerčeva 5, P.O. Box 537, SI-1001 Ljubljana, Slovenia

Received 3 July 2000; received in revised form 25 August 2000; accepted 11 September 2000

Abstract

This study presents a semi-empirical kinetic model for the prediction of monomer conversion and average molecular weight during pseudo-living radical polymerization of methyl methacrylate with tetraphenyl biphosphine as the initiator in bulk, using UV light as the energy source. The model incorporates the chain-transfer to the initiator, which has been shown to be an important reaction for controlling the molecular weight of formed polymers. To solve the set of proposed kinetic equations the method of statistical moments was employed. The kinetic parameters estimated by fitting the initiator conversion data and monomer conversion data were used for modeling the molecular weight profiles, which were in a fair agreement with the experimentally measured average molecular weights.

The pseudo-living radical polymerization scheme is characterized by having reversible termination steps. The proposed circular reaction mechanism was lumped in the empirical power-law reaction rate expression, which seemed to be successfully employed in the model development. The modeling results may be used for the characterization of the polymerization process studied as well as for the prediction of the polymerization behavior at monomer conversions up to 30%.

Keywords: Kinetic modeling; Pseudo-living polymerization; Tetraphenyl biphosphine

1. Introduction

Radical polymerization has generated considerable interest and research in macromolecular chemistry and remarkable progress has been made in this field [1]. Goals in macromolecular research are to increase functionality, improve processing, generate less material waste and reduce cost. These objectives can be achieved by the synthesis of new polymers with well-defined chemical structures, monodispersity of molecular weights, controlled stereochemistry and cross-linking as well as many other structural features. Living anionic and cationic polymerization provides a maximum degree of control and is of considerable importance for the synthesis of polymers with predictable, well-defined structures. Thus, it is not surprising that many efforts in polymer synthesis continue to be directed towards the development of new living polymerization systems. These include a variety of mechanistic types such as anionic, cationic, radical, coordinative, ring-opening and group-transfer polymerization methods [2].

Living-radical polymerization has been difficult to control at the level attained for living ionic polymerizations [3], but the greater versatility of free-radical polymerization and co-polymerization compared to ionic polymerizations somewhat compensates for this deficiency [4]. Free-radical polymerization can be conducted over a wide temperature range, using a variety of solvents, which can be applied to a wide variety of monomers.

In the development of living-radical polymerization, two approaches have been used. The first involves physical prevention of contact between radicals, which prevents the termination. The other involves a repeated reinitiation of polymer growth by thermolysis or photolysis of weak linkages like S–S or P–P bonds, which are incorporated into or at the end of the polymer chain. This method of polymerization is sometimes called pseudo-living [5,6], quasi-living [7], immortal [8], truly living [9], or living polymerization enhancement [10]. Any process that limits radical recombination reduces the rate of termination and as such can result in living polymerization behavior. Another criterion for living-radical polymerization is the ability of the polymer, which has been isolated from the first step of polymerization, to be used as a macroinitiator for the second step of polymerization in which block copolymers or grafted polymers are ultimately formed [4]. Due to their ability to undergo further polymerization, these types of polymers can also be called 'reactive polymers'. The possibility of

---

* Corresponding author. Tel.: +386-1-4760-429; fax: +386-1-4760-425.
E-mail address: matjaz.krajnc@uni-lj.si (M. Krajnc).

0032-3861/01/$ - see front matter © 2001 Elsevier Science Ltd. All rights reserved.
PII: S0032-3861(00)00689-3

Nomenclature

C_{I}^{0}	initial concentration of initiator (mol l^{-1})
C_{mm}	concentration of macromolecules (mol l^{-1})
f	initiator efficiency
i	index
[I]	concentration of initiator (mol l^{-1})
$I_{-\mathrm{OCH}_3}$	proton intensity of $-\mathrm{OCH}_3$ group
$I_{-\mathrm{PPh}_2}$	proton intensity of $-\mathrm{PPh}_2$ group
k	index
k_{d}	apparent dissociation rate constant, mol $^{0.5}$ $\mathrm{l}^{-0.5}$ s^{-1}
k_{i}	initiation rate constant (l mol^{-1} s^{-1})
k_{p}	propagation rate constant (l mol^{-1} s^{-1})
k_{t}	termination rate constant (l^{2} mol^{-2} s^{-1})
k_{tc}	combination rate constant (l mol^{-1} s^{-1})
k_{td}	disproportionation rate constant (l mol^{-1} s^{-1})
k_{tp}	primary radical termination rate constant (l mol^{-1} s^{-1})
$k_{-\mathrm{tp}}$	rate constant (s^{-1})
k_{tr}	chain-transfer rate constant ($\mathrm{l}^{0.5}$ $\mathrm{mol}^{-0.5}$ s^{-1})
m_{p}	mass of polymer (g)
[M]	monomer concentration (mol l^{-1})
M_{I}	molecular weight of initiator
M_{M}	molecular weight of methyl methacrylate
$\bar{M}_{\mathrm{n}}$	number average molecular weight
$\bar{M}_{\mathrm{w}}$	weight average molecular weight
n	reaction order
$\bar{P}_{\mathrm{n}}$	number average degree of polymerization
$[\mathrm{RM}_i^{\cdot}]$	macroradical concentration (mol l^{-1})
$[\mathrm{RM}_i\mathrm{R}]$	concentration of dead polymers (mol l^{-1})
$-r_{\mathrm{d}}$	dissociation rate of the initiator (mol l^{-1} s^{-1})
$-r_{\mathrm{i}}$	initiation rate (mol l^{-1} s^{-1})
$-r_{\mathrm{p}}$	rate of propagation (mol l^{-1} s^{-1})
$-r_{\mathrm{t}}$	termination reaction rate (mol l^{-1} s^{-1})
$-r_{\mathrm{tr}}$	chain-transfer reaction rate (mol l^{-1} s^{-1})
t	reaction time (s)
V	volume of reaction mixture (l)
λ	moment of live polymers
μ	moment of dead polymers

designing optimal material properties by using the appropriate grafted block structures suggests a tremendous commercial potential whereby both block and grafted copolymers have achieved considerable industrial importance. Nevertheless, in contrast to ionic technique, the synthesis of block or grafted copolymers via radical mechanism has several important advantages, e.g. wide choice of monomer combinations and less sensitivity to impurities [11].

Employing iniferters with weak S–S or P–P bonds as initiators may lead to the formation of macroinitiators, which are capable of forming block or grafted copolymers. The use of tetraphenyl biphosphine (TPhBP) as an iniferter in the radical polymerization of methyl methacrylate (MMA) has been studied extensively [12]. The exact mechanism and causes for some discrepancies in the expected molecular weight distribution and polydispersity are still under investigation. Due to the complex reaction scheme of the polymerization studied, the kinetic models proposed in literature do not successfully predict the behavior of the process [13–19].

Kinetic modeling provides an invaluable tool for a polymer chemist and engineer. It allows the prediction of the effects of experimental variables on polymerization, thus limiting the number of time-consuming and expensive experiments that need to be carried out in developing a polymerization process [20]. Polymerization process modeling can be relatively simple if only one deviation from the ideal living system is considered. However, radical polymerization involves several elementary reactions, and therefore a pure analytical solution is not possible. On the other hand, oversimplification may lead to incorrect conclusions.

The aim of this work was to study the kinetics of the synthesis of functionalized MMA macroinitiators with controlled polymerization in bulk, using a TPhBP iniferter. The latter forms radicals that can both initiate the polymerization and react reversibly by growing polymer chains to produce polymers but without narrow polydispersity [21]. The analysis included the deficiencies of the initiation and termination steps studied and the influence of the different model variables on the monomer conversion and average molecular weights. A kinetic model for the prediction of the pseudo-living polymerization of MMA with TPhBP is proposed in order to estimate the monomer conversion as well as molecular weight averages at low conversion conditions. The method of molecular weight moments was employed [13–16,19,22,23]. To estimate the rate constants of the proposed kinetic model the limited set of experimental data [12] was used.

2. Kinetic model

According to the analysis of the experimental data [12], the reaction scheme was predicted as shown in Fig. 1. The initial reaction mixture comprises TPhBP and monomer — MMA. The initiator TPhBP (A) dissociates under the influence of UV light into two radicals $\mathrm{Ph_2P^{\cdot}}$ (B), and reacts with MMA to form MMA free-radicals (C), which start the chain growth. At the end of the polymerization the macroradical (D) terminates in three possible ways to form polymethyl methacrylate (PMMA) macroinitiator products: E, termination by primary radical, chain-transfer to initiator, F, termination by recombination and G + H, termination by disproportionation. The end-group linkage formed is photochemically unstable, and undergoes reversible homolysis to regenerate the propagating radical. For this reason, a circular reaction mechanism, which is a reversible process and is retarded by high concentrations of the initiator, was

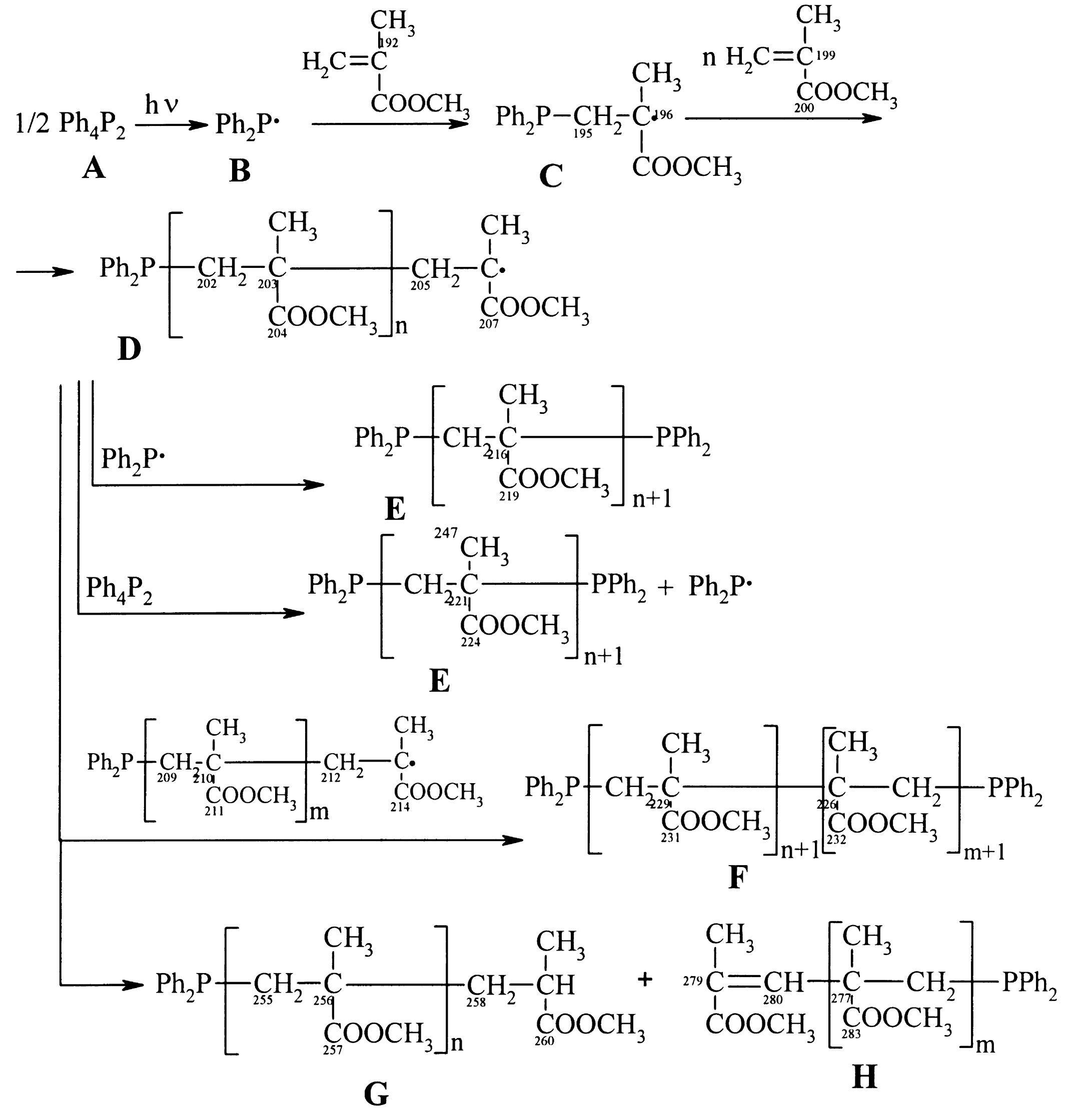

Fig. 1. Reaction scheme of the MMA polymerization with TPhBP.

proposed [12]. The proposed kinetic scheme of polymerization considered in this work is summarized in Table 1, where I is the initiator, $R^{\cdot}$ is the primary radical, $RM_i^{\cdot}$ is the live polymer radical with i repeating units and with one active end-group, $RM\mathit{i}R$, $RM(i+j)R$ are the dead polymers with i or $i+j$ repeating units and with two active end-groups and RM_i, RM_j are the dead polymers with i or j repeating units and with one active end-group.

Photochemical decomposition usually takes place at lower temperatures and is therefore easier to control. The mechanism of the initiator decomposition depends on the bond length, bond energy, and bond order. UV light always decomposes the weakest bonds of the activated initiator depending on the wavelength of the light used. The polymerization reaction takes place under UV light. Consequently, the rate of dissociation of the initiator is difficult to determine as it depends on the intensity of UV light only. However, it was observed that the dissociation of the TPhBP is also concentration dependent. Moreover, although the dissociation of the initiator is usually presented as a first order reaction, the structure of the initiator and analysis of formed products point to a more complex mechanism. For this reason the rate of dissociation of the initiator is presented in an apparent n-power form

$$-r_{\mathrm{d}} = k_{\mathrm{d}}[\mathrm{I}]^n, \tag{1}$$

where k_{d} is an apparent rate constant that is assumed to depend on UV intensity.

It is generally accepted that quasi-steady-state assumption (QSSA) can be applied to the initiator radicals ($R^{\cdot}$) formed by the decomposition of the initiator (a). Assuming that the rate of initiator dissociation (Eq. (1)) is a rate limiting step, the rate of initiation is simplified as shown in the following equation [14,17,18,24]

$$-r_{\mathrm{i}} = 2fk_{\mathrm{d}}[\mathrm{I}]^n. \tag{2}$$

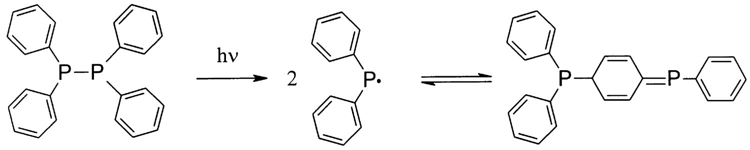

Fig. 2. Photo-dissociation–recombination equilibrium of TPhBP.

It has been found experimentally that not all primary radicals, $R^{\cdot}$, lead to propagation due to waste side reactions. Therefore, the initiator efficiency, *f*, represents the fraction of primary radicals utilized in the chain growth. One of the side reactions is the photo-dissociation–recombination equilibrium of TPhBP, which has been proved to dissociate into two diphenyl phosphine radicals. The diphenyl phosphine radical can further react to undissociated form as the semi-benzene structure (Fig. 2).

The polymerization of MMA with TPhBP was studied at low conversions where no diffusion limitations occur [18,25,26]. Consequently, the propagation rate constant remains unchanged for the whole polymerization process at the conditions under investigation, leading to the propagation rate equation

$$-r_{\mathrm{p}} = k_{\mathrm{p}}[\mathrm{M}][\mathrm{RM}_i^{\cdot}]. \tag{3}$$

The propagation is a repeating incorporation (decomposition of the weakest bond) of new monomers between the chain and the terminated end-groups. The decomposition of the end-groups depends on the bond length, bond energy and bond order of the individually activated bonds and takes place at the weaker bond. The polymer chain must dissociate into a reactive propagating radical and a less reactive radical in order to enable the successive insertion of monomer molecules into the dissociated bond. The rate of polymer chain decomposition is incorporated in the termination-rate expression (Eq. (5)).

Table 1
Proposed kinetic scheme

(1) Initiation	
$\mathrm{I} \xrightarrow{k_{\mathrm{d}}} 2\mathrm{R}^{\cdot}$	(a) homolytic scission
$\mathrm{R}^{\cdot} + \mathrm{M} \xrightarrow{k_{\mathrm{i}}} \mathrm{RM}^{\cdot}$	(b) radical initiation
(2) Propagation	
$\mathrm{RM}_i^{\cdot} + \mathrm{M} \xrightarrow{k_{\mathrm{p}}} \mathrm{RM}_{(i+1)}^{\cdot}$	(c)
(3) Transfer to initiator	
$\mathrm{RM}_i^{\cdot} + \mathrm{I} \xrightarrow{k_{\mathrm{tr}}} \mathrm{RM}_i\mathrm{R} + \mathrm{R}^{\cdot}$	(d)
(4) Termination	
$\mathrm{RM}_i^{\cdot} + \mathrm{RM}_j^{\cdot} \xrightarrow{k_{\mathrm{tc}}} \mathrm{RM}_{(i+j)}\mathrm{R} \underset{k_{\mathrm{tp}}}{\overset{k_{-\mathrm{tp}}}{\rightleftarrows}} \mathrm{RM}_{(i+j)}^{\cdot} + \mathrm{R}^{\cdot}$	(e) recombination
$\mathrm{RM}_i^{\cdot} + \mathrm{RM}_j^{\cdot} \xrightarrow{k_{\mathrm{td}}} \mathrm{RM}_i + \mathrm{RM}_j \underset{k_{\mathrm{tp}}}{\overset{k_{-\mathrm{tp}}}{\rightleftarrows}} \mathrm{R}^{\cdot} + \mathrm{M}_i^{\cdot}$	(f) disproportionation
$\mathrm{RM}_i^{\cdot} + \mathrm{R}^{\cdot} \xrightarrow{k_{\mathrm{tp}}} \mathrm{RM}_i\mathrm{R} \underset{k_{\mathrm{tp}}}{\overset{k_{-\mathrm{tp}}}{\rightleftarrows}} \mathrm{RM}_i^{\cdot} + \mathrm{R}^{\cdot}$	(g) termination by primary radical

One of the possible polymerization steps is also a transfer to the active site from one macromolecule to another molecule. The effect of transfer agent may be determined by plotting the reciprocal value of the degree of polymerization (1/DP) versus molar ratio of transfer agent to monomer. Assuming that the concentration of initiator is constant at low conversions, a plot in Fig. 3 indicates that transfer to initiator is an important step in the polymerization kinetics. Due to the complex mechanism of the initiator dissociation, the rate of chain-transfer to the initiator is also assumed to depend on the initiator concentration in *n*-power, and is expressed in the following form

$$-r_{\mathrm{tr}} = k_{\mathrm{tr}}[\mathrm{I}]^n[\mathrm{RM}_i^{\cdot}]. \tag{4}$$

Pseudo-living radical polymerization schemes are characterized by having thermally or photo-chemically reversible termination steps. Thus, formed macromolecule $\mathrm{RM}_i\mathrm{R}$ is the polymer chain that has been reversibly terminated by phosphine end-group, referred to as the 'living polymer chain' to distinguish it from the growing polymer chain, $\mathrm{RM}_i^{\cdot}$. Consequently, $k_{-\mathrm{tp}}$ is the rate constant of homolytic cleavage of the C–P bond, to give a growing chain-radical and a diphenyl phosphine radical. The termination steps (e and f) together with reversible reactions and primary radical termination (g) were lumped to semi-empirical rate equation giving the final form

$$-r_{\mathrm{t}} = k_{\mathrm{t}}[\mathrm{I}][\mathrm{RM}_i^{\cdot}]^2, \tag{5}$$

where k_{t} is an apparent rate constant that incorporates the influence of different reversible reaction steps to the termination rate. Preliminary calculations of experimental data [12] also showed that the lumped rate of termination is a linear function of the initiator concentration due to the retarding effect of the initiator on the reversible reactions.

The most direct method to solve the set of the proposed kinetic equations (Eqs. (1)–(5)) is to numerically integrate the differential mass balance equations derived directly from the kinetic equations. One has to postulate that the polymer chain does not grow beyond a certain number of monomer units in order to reduce the problem into a finite set of differential equations [24]. The second method is to

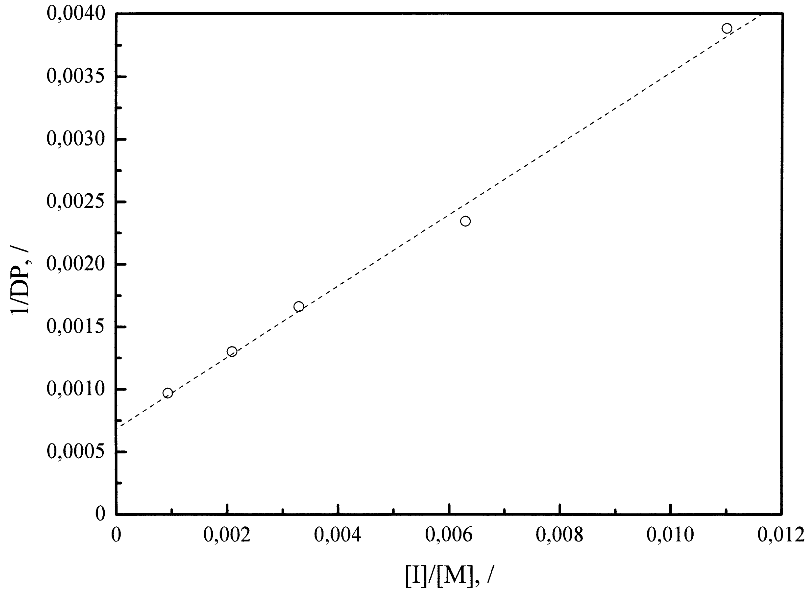

Fig. 3. Determination of initiator chain-transfer.

construct a set of ordinary differential equations (ODEs) based on statistical moments of molecular weights [6]. The method of moments gives some valuable and accurate information from a reduced set of equations and much simplified mathematics. It is perhaps the most widely used method in the modeling of polymerization reactions. The idea is to combine the infinite set of unknowns into a family of polynomials called the moments of the generating function. For the calculation of molecular weight, the following molecular weight moments are defined for live and dead polymers

$$\lambda_k = \sum_{i=1}^{\infty} i^k [\mathrm{RM}_i^{\cdot}], \tag{6}$$

$$\mu_k = \sum_{i=1}^{\infty} i^k [\mathrm{RM}_i\mathrm{R}], \tag{7}$$

where λ_k and μ_k denote the k-th moment of live and dead polymers, respectively. It follows that λ_0 is the total radical concentration and μ_0 is the total concentration of dead polymers, while $\lambda_1 + \mu_1$ is the number of moles of monomer which has reacted.

The number average and weight average polymer molecular weights are defined as [16]

$$\bar{M}_\mathrm{n} = M_\mathrm{M}\frac{\mu_1 + \lambda_1}{\mu_0 + \lambda_0} \cong M_\mathrm{M}\frac{\mu_1}{\mu_0}, \tag{8}$$

$$\bar{M}_\mathrm{w} = M_\mathrm{M}\frac{\mu_2 + \lambda_2}{\mu_1 + \lambda_1} \cong M_\mathrm{M}\frac{\mu_2}{\mu_1}. \tag{9}$$

The complete set of ODEs derived from the kinetic scheme is obtained using the material balance according to the mass action law in terms of the moments of live and dead polymer distributions

$$\frac{\mathrm{d}[\mathrm{M}]}{\mathrm{d}t} = -k_\mathrm{p}[\mathrm{M}]\lambda_0, \tag{10}$$

$$\frac{\mathrm{d}\lambda_0}{\mathrm{d}t} = 2fk_\mathrm{d}[\mathrm{I}]^n - k_\mathrm{t}\lambda_0^2[\mathrm{I}], \tag{11}$$

$$\frac{\mathrm{d}\lambda_1}{\mathrm{d}t} = 2fk_\mathrm{d}[\mathrm{I}]^n + k_\mathrm{p}[\mathrm{M}]\lambda_0 + k_\mathrm{tr}[\mathrm{I}]^n(\lambda_0 - \lambda_1) - k_\mathrm{t}\lambda_0\lambda_1[\mathrm{I}], \tag{12}$$

$$\frac{\mathrm{d}\lambda_2}{\mathrm{d}t} = 2fk_\mathrm{d}[\mathrm{I}]^n + k_\mathrm{p}[\mathrm{M}](2\lambda_1 + \lambda_0) + k_\mathrm{tr}[\mathrm{I}]^n(\lambda_0 - \lambda_2) - k_\mathrm{t}\lambda_0\lambda_2[\mathrm{I}], \tag{13}$$

$$\frac{\mathrm{d}\mu_0}{\mathrm{d}t} = (k_\mathrm{td} + 0.5k_\mathrm{tc})\lambda_0^2[\mathrm{I}] + k_\mathrm{tr}[\mathrm{I}]^n\lambda_0, \tag{14}$$

$$\frac{\mathrm{d}\mu_1}{\mathrm{d}t} = k_\mathrm{t}\lambda_0\lambda_1[\mathrm{I}] + k_\mathrm{tr}[\mathrm{I}]^n\lambda_1, \tag{15}$$

$$\frac{\mathrm{d}\mu_2}{\mathrm{d}t} = k_\mathrm{t}\lambda_0\lambda_2[\mathrm{I}] + k_\mathrm{tc}\lambda_1^2[\mathrm{I}] + k_\mathrm{tr}[\mathrm{I}]^n\lambda_2, \tag{16}$$

where λ_0, λ_1, λ_2 and μ_0, μ_1, μ_2 are the zero, first and second moment of the live and dead polymer molecular weight distributions, respectively. Derivation of the above equations can be found in literature [6,13–19]. The kinetic model was solved by simultaneously integrating mass balance equation derived from Eqs. (1) and (10)–(16).

3. Experimental

3.1. Materials

MMA, a product of Aldrich and Rohm and Haas was washed with a 10% solution of sodium carbonate and distilled water, dried over night with non-aqueous sodium sulphate, distilled twice under reduced pressure, and then purged with argon to remove oxygen. Monomer was used immediately after the purification. TPhBP (Aldrich) was used as the initiator. All solvents used for the precipitation were dried, purified and distilled twice in dry argon to remove all oxygen.

3.2. Synthesis of macroinitiators

The experimental setup and procedure are described in detail in our previous work [12]. Bulk polymerizations of MMA were carried out in a dry box purged with argon. The content of oxygen and water in argon was below 1 ppm. At the reaction temperature 25°C the monomers were mixed in a quartz reaction vessel with a selected quantity of TPhBP. The initiator concentration varied between 0.0178 and 0.0893 mol dm^{-3}. Molar ratio of monomer to initiator varied from 1:0.002 to 1:0.01. The polymerization time was between 1 and 4 h. A UV lamp of 366 nm wavelength with an intensity of 4.5 mW cm^{-2} at 2.5 cm distance was used as the energy source for polymerization. The samples for determining the monomer conversion and molecular weight of polymerization were withdrawn from the reaction vessel at selected reaction-time intervals. All samples of the PMMA were precipitated three times at room temperature in a dry box with argon atmosphere from tetrahydrofuran solution into methanol to remove the unreacted initiator and monomer, and were dried successively for 8 h in vacuum at room temperature. Under the same reaction conditions two control experiments were carried out. To evaluate the degree of thermal and photo polymerization, the reaction with TPhBP without UV irradiation for thermal and without TPhBP with UV irradiation for photo polymerization were carried out as well. In both cases the monomer conversion did not exceed 1%.

3.3. Determination of structure and molecular weight

The ^{1}H and ^{31}P spectra were measured with Bruker DPX 300 MHz and Varian INOVA 600 MHz NMR spectrometers in one and two dimensional technique with homo

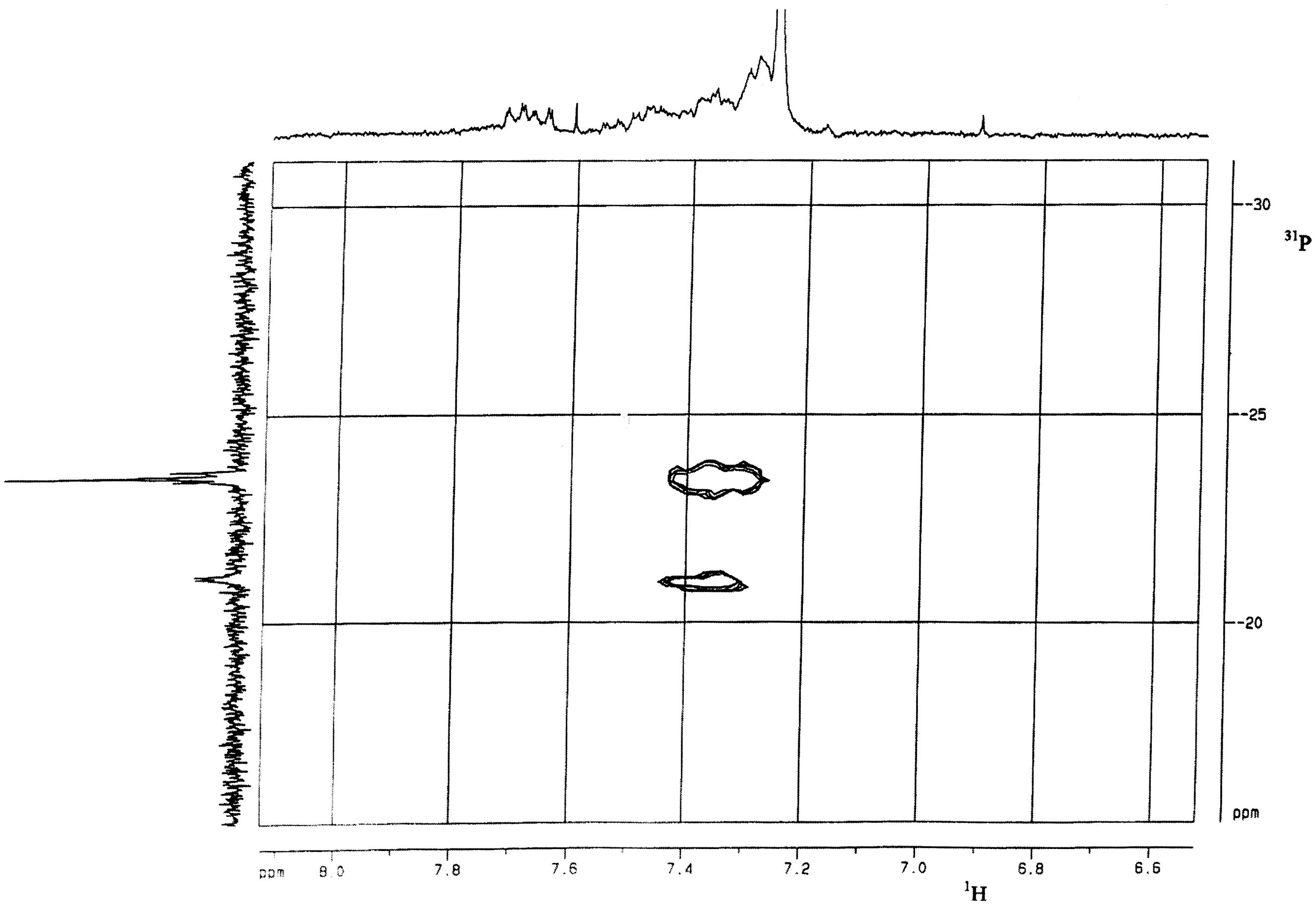

Fig. 4. HETCOR ^{1}H–^{31}P NMR spectrum of the PMMA.

and hetero correlation. $CDCl_3$ was used as the solvent. The samples were sealed to NMR tubes in a dry box with argon atmosphere to prevent oxidation of phosphine end-groups. All ^1H signals were quoted on tetramethylsilane as an internal standard. The molecular weights of PMMA were determined from the ratio of end-group signals of PMMA versus the signals of the chain in the ^1H NMR spectra. Molecular weights were also measured by GPC on PL-gel columns with pore sizes 50, 100 and 1000 nm. Tetrahydrofuran was used as an eluent. Narrow molecular weight distribution PMMA standards were used for column calibration. The purity of polymers was controlled by ^{31}P NMR measurements of the macromolecule end-groups and of the unreacted initiator.

4. Results and discussion

For the determination of molecular weights, GPC and ^1H NMR were used as two independent methods. For the final products, the molecular weights for PMMA were calculated from the ratio of integrals of aromatic proton signals of the end-groups between 7.2 and 7.6 ppm versus signals of the chain, with the assumption that each macromolecule contained two non-oxidized phosphine end-groups with two phenyl groups. This assumption was made on the basis of the observed spectra and determined signal intensities from ^1H and ^{31}P NMR spectra and two-dimensional (2D) homo and hetero correlation spectra of PMMA (Fig. 4). For the identification of the end-group, phosphorus spectra of PMMA were used. In the ^{31}P proton decoupling spectra of PMMA the phosphine head and tail end-groups showed strong signals at −21.1 and −23.5 ppm, respectively. The structure of the end-groups can also be assigned by measuring the inserted phosphorus atom between the end-group and the rest of the macromolecule. In the case of the $-CH_2P(Ph)_2$ group, the P atom prevented space or bond coupling between $-CH_2-$ and $-Ph$ protons, while in the case of $-CH_2Ph$ groups the proton long-range coupling should be seen. Due to the inserted phosphorous atom between the chain and the end-group, there was no space or bond coupling between the end-groups and the rest of the macromolecule, which would be expressed as out-of-diagonal signals in the spectra, in COSY H–H and NOESY H–H spectra [12].

The measurements of the relative intensity of $-P(Ph_2)$ end-group proton signal against the monomer unit $-OCH_3$ proton signal at 3.60 ppm, provides the $\bar{M}_n$ [27]

$$\bar{M}_n = \frac{I_{OCH_3}}{I_{PPh_2}} \times \frac{20}{3} \times M_M + M_I, \tag{17}$$

where the value 20/3 represents the proton ratio of the two active end-groups $-P(Ph_2)$ versus the $-OCH_3$ group. The calculated molecular weights of final products were compared with those observed by GPC. In spite of the different principle of measurements the agreement between the results is satisfactory, within ±10% error.

In general terms, the QSSA states that the rate of radical initiation is approximately equal to the rate of radical termination [14]. Consequently, the number of chains formed can be estimated from the molecular weight of the polymer. It was assumed that each macromolecule has two biphenyl phosphine end-groups at the end of the chain. The average concentration of macromolecules (C_{mm}) at individual reaction times can therefore be approximated from the mass of polymer (m_p) and the average molecular weight ($\bar{M}_n$) by the following relationship

$$C_{mm} = \frac{m_p}{\bar{M}_n} \frac{1}{V}. \tag{18}$$

The rate of initiation was determined from the slope of concentration-time data of the macromolecules formed.

Assuming that each macromolecule contains one molecule of initiator, the initiator concentration may be estimated from polymer concentration using the expression

$$[I] = C_I^0 - C_{mm}, \tag{19}$$

where C_I^0 is initial concentration of initiator.

Knowing the rate of initiation and the initiator concentration profile the dissociation constant (k_d), the reaction order n of the initiator dissociation rate (Eq. (1)) and the efficiency factor, f, may be determined using the QSSA. The kinetic parameters for dissociation and initiation reaction rates were optimized by fitting the integrated mass balance equation derived from Eq. (1) and initiation rate equation (Eq. (2)) to experimental results employing a simplex method. The results are presented in Table 2. The excellent agreement between calculated and experimental data is shown in Fig. 5. It can be observed from the results that the rate of initiator dissociation does not follow the first order kinetic. The apparent 0.5 reaction order may be ascribed to a complex mechanism of initiator decomposition.

The value of the propagation constant, k_p, $180\ l\ mol^{-1}\ s^{-1}$ was adopted for the experimental conditions used in the polymerization system studied [28]. To determine the termination constant, k_t, the ratio k_{td}/k_{tc} of 7/3 was used [26].

The determination of termination (k_t), and transfer (k_{tr}) constant values was performed by fitting the evaluated kinetic model, using a limited set of monomer conversion experimental data. A semi-implicit fourth-order Runge–Kutta algorithm with stiffness was used for ODEs integration. Both constants were simultaneously estimated by using the nonlinear regression technique based on

Table 2
Estimated kinetic parameters for the methyl methacrylate polymerization

$n(/)$	0.5
$f(/)$	0.50 ± 0.05
k_d ($mol^{0.5}\ l^{-0.5}\ s^{-1}$)	$(2.42 \pm 0.29) \times 10^{-6}$
k_{tr} ($l^{0.5}\ mol^{-0.5}\ s^{-1}$)	2.09 ± 0.21
k_t ($l^2\ mol^{-2}\ s^{-1}$)	$(6.53 \pm 0.20) \times 10^8$

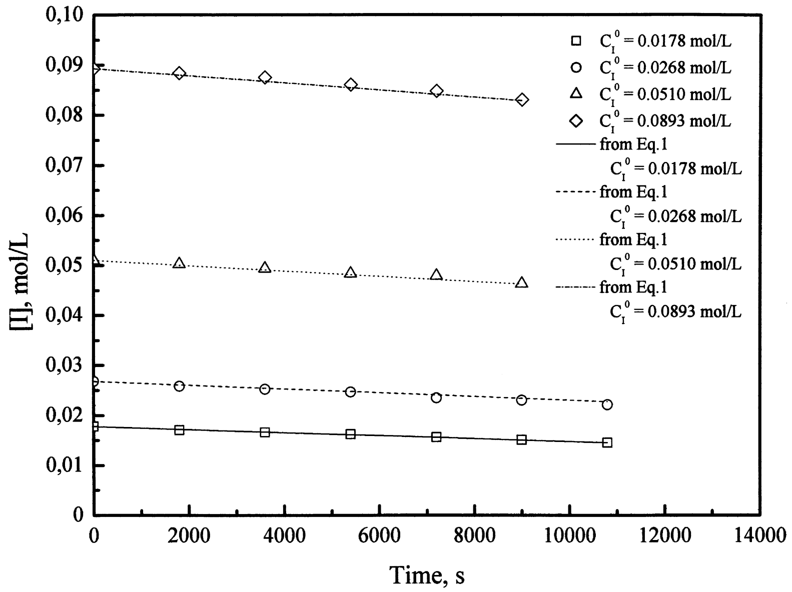

Fig. 5. Initiator concentration profiles.

Levenberg–Marquardt algorithm [29]. Table 2 shows the results of the parameter estimation at 95% confidence interval. Since the experimentally measured conversions were relatively low, the influence of diffusion limitations on the kinetic constants was neglected.

The average molecular weights, polydispersity, and monomer conversions may be calculated from the kinetic model by using optimized kinetic parameters. The comparison of the calculated and experimental data representing the monomer conversion is illustrated in Fig. 6. Similarly, average molecular weight versus time is represented in Fig. 7. The calculated $\bar{M}_n$ was determined from the solution of the model by using Eq. (8). In general, there is a fair agreement between predicted and experimental values of monomer conversion as well as average molecular weight. At higher values, the discrepancies between predicted and experimental values of conversion were observed which may be due to the increasing effect of diffusion limitations, which was not incorporated in the kinetic model.

The calculated polydispersities at different initial concentrations of initiator varied between 1.96 and 1.98 in all runs,

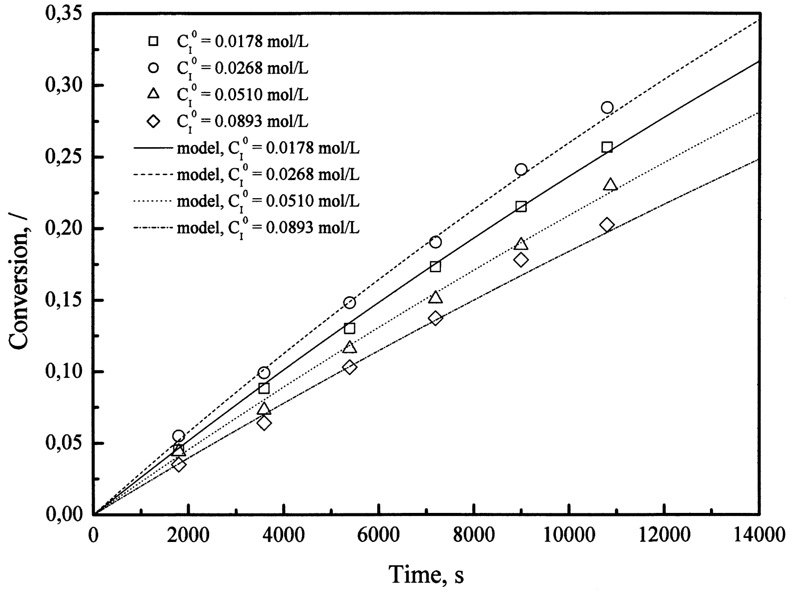

Fig. 6. Conversion of MMA at different initial concentrations of initiator.

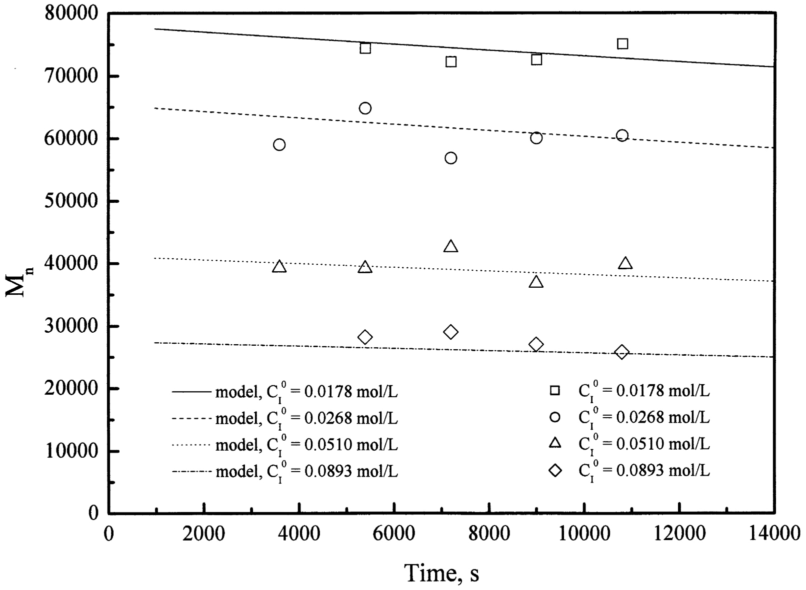

Fig. 7. Average molecular weight at different initial concentrations of initiator.

which is in good agreement with experimental results between 1.8 and 2.4 [12].

From the analysis of the kinetic model developed, it may be concluded, that the reinitiation is rapid and changes in the propagation rate are not observed. The same number of monomer molecules is consumed per unit time with the formation of a larger number of smaller-sized polymer molecules. Consequently, the average molecular weight strongly depends on the chain-transfer constant. On the other hand, it is much less dependent on the changes of termination constant values due to circular reaction mechanism. It was also found that k_t and k_{tr} changes have no effect on the polydispersity.

5. Conclusions

The semi-empirical kinetic model for the prediction of monomer conversion and average molecular weight during the pseudo-living radical polymerization of MMA was developed. The model incorporates the chain-transfer to initiator, which has been shown to be an important reaction for controlling the molecular weight of formed polymers.

The increase in the initiator concentration decreases the propagation rate due to the retarding effect of the initiator on reversible reaction steps. The proposed circular reaction mechanism was lumped in the empirical power-law reaction rate expression, which seemed to be successfully employed in the model development. The kinetic model does not take into account diffusion limitations. The modeling results may be used for the characterization of the polymerization process studied as well as for the prediction of the polymerization behavior at monomer conversions up to 30%.

By comparison of the model and experimental results it can be assumed that the mechanism of pseudo-living radical polymerization and the dissociation of TPhBP are complex processes with several intermediary steps which the suggested reaction scheme does not take into account. Through the development of the kinetic model of polymerization of MMA with TPhBP some insight into the mechanism of specific radical polymerization has been gained.

References

[1] Matyjaszewski K. Controlled radical polymerization, Symposium Series, 685. Washington, DC: American Chemical Society, 1998 (p. 396–417).
[2] Quirk RP, Bumjae L. Polym Int 1992;27:359–67.
[3] Greszta D, Matyjaszewski K. Macromolecules 1996;29:7661–70.
[4] Harwood HJ. Encyclopedia of polymer science and engineering, Suppl vol. New York: Wiley/Interscience, 1990.
[5] Ferington TE, Tobolsky AV. J Am Chem Soc 1955;77:4510–2.
[6] Baillagou PE, Soong DS. Chem Engng Sci 1985;40:87–104.
[7] Otsu T. J Polym Sci 1957;26:236–9.
[8] Otsu T, Ogawa T, Yamamoto T. Macromolecules 1986;19:2087–9.
[9] Reghunadhan NCP, Clouet G. Macromol Chem 1989;190:1243–52.
[10] Endo K, Murata K, Otsu T. Macromolecules 1992;25:5554–6.
[11] Düz AB, Önen A, Angewandte Yağci Y. Makromol Chem 1998;258:1–4.
[12] Poljanšek I, Šebenik A. Macromol Chem Phys 1999;200:2088–99.
[13] Louie BM, Carrat GM, Soong DS. J Appl Polym Sci 1985;30:3985–4012.
[14] Venkateshwaran G, Kumar A. J Appl Polym Sci 1992;45:187–215.
[15] Benedicto AD, Claverie JP, Grubbs RH. Macromolecules 1995;28:500–11.

[16] Crowley TJ, Choi KY. Ind Engng Chem Res 1997;36:1419–23.

[17] Tefera N, Weickert G, Westerterp KR. J Appl Polym Sci 1997;63:1649–61.

[18] Tefera N, Weickert G, Westerterp KR. J Appl Polym Sci 1997;63:1663–80.

[19] Fenouillot F, Terrisse J, Rimlinger T. Int Polym Process 1998;13:154–61.

[20] Johnson CHJ, Moad G, Solomon DH, Spurling TH, Vearing DJ. Aust J Chem 1990;43:1215–30.

[21] Otsu T, Yoshida M. Macromol Chem, Rapid Commun 1982;3:127–32.

[22] Butté A, Storti G, Morbidelli M. Chem Engng Sci 1999;54:3225–31.

[23] Shi AC, Georges MK, Mahabadi HK. Polym Reaction Engng 1999;7(2):283–300.

[24] Chaimberg M, Cohen Y. Ind Engng Chem Res 1990;29:1152–60.

[25] Huang YJ, Fan JD, Lee LJ. J Appl Polym Sci 1987;33:1315–41.

[26] Achilias D, Kiparissides C. J Appl Polym Sci 1988;35:1303–23.

[27] Hatada K, Kitayama T, Vogl O. Macromolecular design of polymeric materials. New York: Marcel Dekker, 1997.

[28] Brandrup J, Immergut EH, Grulke EA. Polymer handbook. 4th ed. New York: Wiley/Interscience, 1999.

[29] Marquardt DW. J Soc Ind Appl Math 1963;11:431–41.